Vibrational Spectra of Linear Oligomers of Carbonic Acid: A Quantum Chemical Study

ARTICLE *in* THE JOURNAL OF PHYSICAL CHEMISTRY A · FEBRUARY 2012

Impact Factor: 2.69 · DOI: 10.1021/jp209715x · Source: PubMed

3 AUTHORS, INCLUDING:

Sandeep Kumar Reddy
University of California, San Diego
12 PUBLICATIONS **160** CITATIONS
SEE PROFILE

Chidambar Kulkarni
Technische Universiteit Eindhoven
15 PUBLICATIONS **223** CITATIONS
SEE PROFILE

THE JOURNAL OF PHYSICAL CHEMISTRY A

Article

pubs.acs.org/JPCA

Vibrational Spectra of Linear Oligomers of Carbonic Acid: A Quantum Chemical Study

Sandeep K. Reddy, Chidambar H. Kulkarni, and Sundaram Balasubramanian*

Chemistry and Physics of Materials Unit, Jawaharlal Nehru Centre for Advanced Scientific Research, Jakkur, Bangalore 560 064, India

Supporting Information

ABSTRACT: Gas phase quantum chemical calculations of linear, hydrogen bonded oligomers of carbonic acid have been carried out to examine the feasibility for such species to be the building blocks of crystalline carbonic acid. Infrared and Raman vibrational spectra have been calculated and are compared against experimentally known spectra for two polymorphs of carbonic acid. The calculated anharmonic frequencies of the linear oligomer agree well with the experimental data for the centrosymmetric β-carbonic acid, rather than with that for the α polymorph. These calculations strongly suggest that β-carbonic acid should consist of one-dimensional hydrogen bonded carbonic acid molecules in the anti−anti conformation.

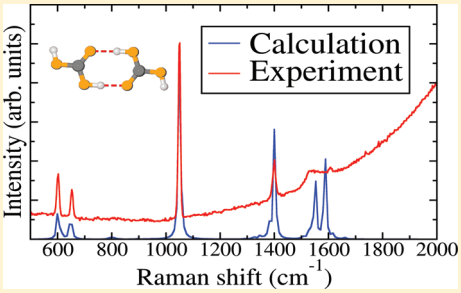

1. INTRODUCTION

Carbonic acid (CA), a small molecule, has deep environmental and astrophysical significance.[1−8] In the presence of water, it dissociates rapidly to carbon dioxide and water. Hence its existence as a stable compound was a matter of uncertainty for many years. Schwarz et al. discovered signatures of this molecule in the decomposition of NH_4HCO_3(s) using mass spectroscopy.[9] It was later synthesized under equilibrium conditions using cryogenic techniques by Hage et al. in 1993.[10] Since then, various experimental and theoretical studies have started to yield crucial pieces of information on this elusive molecule.[3−31]

Two different crystalline polymorphs of this compound have been synthesized, α and β. While the former is obtained by the protonation of a methanolic solution of bicarbonate, the latter is obtained through the same procedure but in an aqueous solution. The two crystals have been characterized through infrared spectroscopy recorded for wave numbers beyond 500 cm^{-1}. Recently, the experimental Raman spectra of the β form has been obtained over a wide range, from 100 to 4000 cm^{-1}.[26,32] The mutual exclusion of Raman and infrared (IR) active modes in the β-polymorph showed that it should contain a center of inversion symmetry.[26] A recent review of the current status of the experimental work can be found in Loerting.[30]

The lack of even density data for these crystals has considerably hindered theoretical studies. Tossell[23] carried out high-quality quantum chemical calculations of the monomer and of the dimeric species in gas phase and compared their vibrational features to the experimental infrared spectra of the polymorphs. He rightly concluded that the dimer spectrum was in closer agreement to experiment than that of the monomer and suggested the presence of oligomeric species in the crystal. While early investigations looked at hydrogen-bonded oligomers as possible species in the solid state,[17] more recent ones employed crystal structure prediction tools.[33,34] Our recent effort used quantum chemical calculations of monomers and dimers as reference to develop a force field for carbonic acid.[34] This force field was employed to obtain crystal structures in many different space groups, which were then sorted based on their lattice energies. The lowest energy structures were further investigated using zero Kelvin periodic density functional theory calculations as well as through density functional theory (DFT) based ab initio molecular dynamics (AIMD) simulations. The central conclusion of this work was that crystals containing one-dimensional hydrogen bonded CA molecules were more stable than those that contain two-dimensional sheet-like hydrogen bond networks. The infrared spectrum calculated from AIMD for such crystals compared well with available experimental data. Our observation that β-carbonic acid could likely consist of one-dimensional chains of hydrogen bonded molecules has been supported by recent low-frequency Raman spectroscopic results of the two polymorphs of CA.[32]

In our earlier work,[34] the Raman spectrum of one of the candidate structures was calculated for a small frequency range around 900 cm^{-1} and was compared against the then available experimental data. In view of the recent experiments of Loerting and co-workers on the low-frequency Raman spectroscopy of solid carbonic acid,[32] it becomes imperative that the vibrational spectra of linear hydrogen-bonded oligomers are obtained using accurate quantum chemical methods. The current work is aimed in this direction. Herein, we have carried out both MP2 and density functional theory based calculations using a hybrid functional to obtain the IR and Raman spectra of gas phase oligomers of carbonic acid and compare them with experimental data.

This paper is divided into four sections. Following this Introduction, we provide the computational methodologies

Received: October 10, 2011
Revised: January 11, 2012
Published: January 12, 2012

Table 1. Energies (in kcal/mol) of Oligomers Calculated at B3LYP/6-311G(2d,d,p) and MP2/6-311G(2d,d,p) Levels of Theory[a]

	B3LYP/6-311G(2d,d,p)		MP2/6-311G(2d,d,p)	
oligomer	without BSSE	with BSSE	without BSSE	with BSSE
a-a monomer	0	0	0	0
dimer a	−17.92	−14.43 (−13.53)	−15.95	−10.63
dimer b	−19.95	−16.69 (−15.44)	−18.43	−13.41 (−11.89)
trimer	−37.98	−31.63 (−29.29)	−35.54	−25.64
tetramer	−56.12	−46.64 (−43.21)	−52.72	−37.93 (−33.82)
pentamer	−74.17	−61.59 (−57.14)	−69.85	−50.16
hexamer	−92.21	−76.51 (−70.96)	−86.96	−62.38
heptamer	−110.26	−90.87 (−84.25)	−104.06	−74.56
octamer	−128.29	−105.67 (−97.99)	−121.16	−86.79

[a]See Supporting Information for oligomer geometries. Values are calculated as $E_n - nE_1$ where E_n is the total energy of the oligomer of size n and E_1 is that for the monomer. Energies are in kcal/mol. Values in parentheses include zero point energy (ZPE) contribution.

adopted. The stability of oligomers is discussed later. The third section is devoted to describe vibrational analyses of the oligomers, ranging from the monomer to octamer (the mode assignments are also presented) and comparison of the vibrational spectrum of the octamer with the experimental infrared (IR) and Raman spectra of the two polymorphs of CA. The last section summarizes the results.

2. COMPUTATIONAL DETAILS

The geometries and vibrational spectra of all oligomers in gas phase were obtained at B3LYP/6-311G(2d,d,p) level of theory using the Gaussian09 code.[35] Because this functional lacks a complete description of electron correlation, geometry optimizations of all oligomers were also carried out at MP2/6-311G(2d,d,p) level of theory. Harmonic vibrational spectra up to a tetramer are obtained at the MP2 level and compared with spectra obtained at B3LYP/6-311G(2d,d,p) level. Initial geometries of the oligomers were modeled using Gaussview. The keywords "Opt=verytight" and "scf=verytight" were employed during optimizations, which limits the root-mean-square of force on the nuclei and on the wave function to 10^{-6} and 10^{-8} a.u., respectively. Further, an ultrafine grid was used in the DFT calculations. Normal mode calculations at the harmonic level showed no imaginary frequency for any of the oligomers.

Binding energy of an oligomer was calculated in two ways. In the first instance, it was defined as

$$\Delta E = E_n - nE_1 \quad (1)$$

Second, it was also defined as the energy gained due to the addition of a molecule to the oligomer, as

$$\Delta E = E_n - E_{n-1} \quad (2)$$

Here n is the size of the oligomeric unit and E_n is its ground state energy.

The optimized geometries of these oligomers were used to calculate the vibrational spectra. Anharmonic frequencies were calculated using second-order perturbation theory as implemented in Gaussian09. Anharmonic frequencies for the pentamer and for larger oligomers were found to exhibit a few imaginary frequencies, although the corresponding frequencies at the harmonic level were all positive. Anharmonic frequencies are calculated by adding corrections to harmonic values using perturbation theory. So these imaginary values could have arisen due to the failure of the anharmonic approximation in the low-frequency region. Here, we call these floppy modes. At the B3LYP/6-311G(2d,d,p) level, we report here harmonic frequencies for oligomers up to the octamer and anharmonic frequencies up to the tetramer. At the MP2/6-311G(2d,d,p) level, harmonic frequencies up to the linear tetramer are reported. We also use scale factors between harmonic and anharmonic frequencies, obtained from the spectrum of the tetramer to estimate anharmonic frequencies for the octamer. Unless specified, all frequencies provided in this paper were not scaled by any factor. The intensity of infrared absorption was calculated by applying a finite difference approximation to calculate the gradient of the dipole moment with respect to the normal mode coordinate. The square of this quantity is proportional to the infrared intensity. Raman intensity was obtained by calculating the polarizability tensor, which is equal to the gradient of the induced dipole moment with respect to the external electric field. The finite difference of this tensor with respect to normal mode coordinates is proportional to the Raman intensity of the mode. It is to be noted that these equations are derived within the harmonic approximation, that is, higher order derivatives of energy, dipole moment, and polarizability with respect to the normal mode coordinate were assumed to be negligible.[36]

The structures were visualized using Gaussview[35] and Jmol.[37,38]

3. RESULTS AND DISCUSSION

Geometry Optimization. Geometry optimization of the three conformers of carbonic acid, namely, anti−anti (a-a), anti−syn (a-s), and syn−syn (s-s), were carried out. Among these, the a-a conformer is the most stable. The a-s and s-s conformers are less stable than the a-a conformer by 1.9016 and 12.167 kcal/mol, respectively, as calculated at the B3LYP/6-311G(2d,d,p) level. These are comparable to the values of 1.74 and 10.9 kcal/mol, calculated at the CCSD(T)/cc-pVTZ level by Endo and co-workers.[28]

Linear oligomers of the a-a conformer up to the size of an octamer were also studied. A dimer of the a-s conformer was also investigated. The structures of these oligomers are given in Figures S1−S5 (see Supporting Information). Two stable dimers are found, dimer a and dimer b. Dimer a consists of two a-s monomers connected to each other through two hydrogen bonds of equal strength, while dimer b consists of two a-a conformers that form two hydrogen bonds of equal strength (Figure S2, Supporting Information). The dimerization energy (i.e., $E_2 - 2E_1$) of dimer b is more negative than that of dimer a by 1.797 kcal/mol. Loerting et al. reported recently that the gas

dx.doi.org/10.1021/jp209715x | J. Phys. Chem. A 2012, 116, 1638−1647

phase of carbonic acid consists of monomers largely (around 90%) in the a-a conformation with the balance being constituted by a-s monomer and dimer b species.[29]

The binding energies of oligomers studied here are provided in Table 1. The number of hydrogen bonds in an oligomer is $2n - 2$ where n is the number of molecules in the oligomer. As n increases, the binding energy, calculated using eq 1, decreases and reaches a saturation value as shown in Figure 1. The

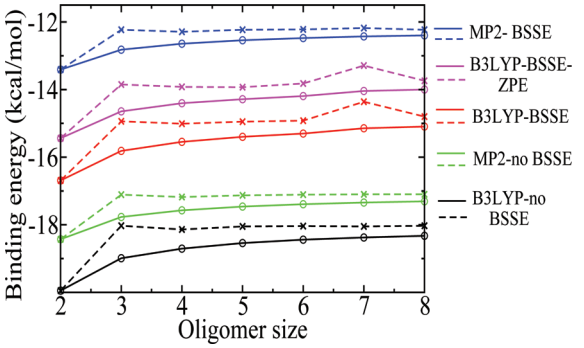

Figure 1. Binding energy of oligomers as a function of oligomer size. Binding energy is calculated in two ways; $E_n - nE_1/(n-1)$ (continuous lines) and $E_n - E_{n-1}$ (dashed lines) where n is the size of oligomer, E_1 is the energy of monomer, and E_n is the energy of nth oligomer.

saturation binding energies thus obtained are −15.3 (−18.45) and −12.47 (−17.40) kcal/mol calculated at B3LYP/6-311G(2d,d,p) and MP2/6-311G(2d,d,p) levels of theory, respectively. Values in parentheses are energies without the basis-set superposition error (BSSE) correction. Specifically for CA, it has earlier been shown that counterpoise correction could overestimate the BSSE in the case of MP2 methods.[15] So, the saturation value of −17.4 kcal/mol obtained here without BSSE compares well with the extrapolated value of −18.3 kcal/mol reported by Liedl et al.[15] for the dimerization energy of CA based on MP2/aug-cc-pVDZ and MP2/aug-cc-pVTZ calculations.

Optimized geometries of all oligomers are provided in Supporting Information.

Vibrational Frequencies. Based on ab initio MD results using the PBE functional, we have recently proposed that linear oligomers of the a-a conformer are likely to be the building blocks for at least one of the crystalline polymorphs of carbonic acid, β.[34] The stability of such oligomeric species as observed in the current accurate gas phase calculations offers further credence to this proposal. Given the fact that the experimental infrared and Raman spectra of the two crystalline polymorphs α and β are available, it becomes important to study the vibrational modes using quantum chemical methods. In the current work, we assume that interchain interactions that could be present in these crystals do not affect the intramolecular vibrational modes, at least the high-frequency ones. In an earlier study of the crystals containing such chain motifs,[34] we had noticed that adjacent chains separated by a distance of 3.1 Å did not affect the vibrational frequencies of a given chain.

The vibrational spectra of CA oligomers in the frequency range 500−4000 cm^{-1} are discussed here. Table 2 shows the harmonic and anharmonic frequencies of the a-a and a-s monomers along with assignments of the modes (see Table S1 of Supporting Information for IR and Raman activities of these modes). The ratio of anharmonic to harmonic frequency of various modes is in the range 0.951−0.994. The largest difference of about 180 cm^{-1} is seen for the O−H stretch. The frequencies obtained from the B3LYP calculations are comparable to those from MP2 calculations. These values are also compared against data reported by Tossell[23] for the a-s monomer. He estimated the anharmonic values at CCSD/6-311+g(2d,p) level of theory by summing the harmonic frequencies at the same level with the difference between harmonic and anharmonic values calculated at B3LYP/6-311g(2d,d,p) level of theory. Our results agree with those of Tossell's. The calculated anharmonic values at the B3LYP/6-311g(2d,d,p) differ by about 20−45 cm^{-1}. This difference is the same as reported by Tossell.[23] Frequencies at the MP2/6-311g(2d,d,p) level are 5−30 cm^{-1} larger compared with the CCSD results.[23] At frequencies below 700 cm^{-1}, the difference is small and the largest variation is observed for the O−H

Table 2. Harmonic and Anharmonic Frequencies (in cm^{-1}) of the anti−anti (a-a) and anti−syn (a-s) Monomers, Calculated at B3LYP/6-311G(2d,d,p) and MP2/6-311G(2d,d,dp) Levels of Theory[a]

a-a				a-s				
B3LYP		MP2		B3LYP		MP2		
har	anhar	har	anhar	har	anhar	har	anhar[b]	assignment
526.5	534.5	526.1	511.6	485.6	472.1	470.9	465.3 (458)	δ_{oop} COH
603.7	596.8	607.9	580.3	568.5	548.6	567.2	540.9 (533)	
550.6	545.7	558.0	552.0	545.4	538.6	556.6	548.8 (550)	δ_{oop} COO
605.8	602.0	610.7	605.9	609.7	604.5	613.4	608.3 (623)	δ_{iop} CO_3
799.6	787.0	802.9	790.3	785.2	773.8	788.9	777.7 (798)	δ_{oop} CO_3
981.1	957.1	994.9	970.2	967.9	933.7	980.3	948.7 (960)	$\nu_s(C(OH)_2)$
1163.7	1109.3	1195.2	1154.8	1152.8	1127.8	1182.3	1142.2 (1159)	$\nu_{as}(C(OH)_2)$ and $\delta_{ip}C(OH)$
1304.6	1259.1	1325.2	1275.6	1274.1	1220.4	1297.4	1248.6 (1253)	$\delta_{ip}C(OH)$ and $\nu(C{=}O)$
1467.5	1429.1	1494.3	1454.4	1407.0	1369.0	1436.1	1395.8 (1408)	$\nu_{as}(C(OH)_2)$
1851.9	1808.8	1885.7	1851.4	1905.1	1846.5	1930.9	1874.2 (1864)	$\nu(C{=}O)$
3812.9	3627.3	3875.6	3690.5	3804.3	3618.7	3875.1	3690.6 (3660)	$\nu(O{-}H)$
3816	3629.6	3878.4	3692.3	3806.6	3617.5	3881.4	3696.4 (3664)	

[a]Mode assignments are also shown. Calculated Raman and infrared absorption activities are provided in Table S1 of Supporting Information. [b]Values in parentheses are estimated anharmonic values reported by Tossell[23] for the a-s monomer, calculated at CCSD/6-311+G(2d,p) level of theory.

dx.doi.org/10.1021/jp209715x | J. Phys. Chem. A 2012, 116, 1638−1647

Table 3. Calculated Harmonic and Anharmonic Frequencies (in cm^{-1}) of the Two Dimers along with Mode Assignments and IR and Raman Intensities of Corresponding Modes (Columns 3 and 6)[a]

dimer a			dimer b			
har	anhar	activity	har	anhar[b]	activity	assignment
572.2	564.3	R(4.6355)	572.7	565.5 (566)	R(1.3)	δ_{ip}(COO)
614.0	608.0	I(4.4817)	604.8	598.1 (598)	I(135.6)	
545.5	546.6	R(5.0585)	576.0	572.7 (573)	R(6.1)	δ_{oop}(COH)
548.8	549.9	I(262.9165)	577.6	574.2 (574)	I(194.2)	
645.7	642.3	R(4.3975)	642.7	639.6 (639)	R(6.4)	$\delta_{ip}(CO_3)$
658.8	655.3	I(14.9854)	653.9	649.5 (648)	I(44.8)	
796.6	787.1	R(0.2267)	802.4	793.5 (794)	R(0.2)	$\delta_{oop}(CO_3)$
798.8	788.9	I(41.6636)	804.0	794.4 (795)	I(43.9)	
936.2	909.6	R(0.3308)	923.9	899.0 (897)	R(0.2)	δ_{oop}(COH)
983.7	962.4	I(207.9773)	971.9	948.2 (947)	I(264.4)	
1021.7	1004.8	I(63.1800)	1025.2	1006.1 (1006)	I (24.3)	$\nu_s(C(OH)_2)$
1031.0	1014.7	R(18.2964)	1031.9	1012.8 (1013)	R(21.8)	
1239.4	1200.6	R(9.0758)	1237.4	1202.3 (1201)	R(2.5)	$\nu_{as}(C(OH)_2)$ and δ_{ip}C(OH)
1246.7	1202.3	I(161.7219)	1242.5	1205.8 (1204)	I(694.4)	
1362.6	1319.9	R(4.0392)	1390.6	1343.0 (1343)	I (280.0)	δ_{ip}(COH) and ν(C═O)
1365.3	1335.8	I(927.6910)	1392.2	1348.7 (1386)	R(6.6)	
1489.0	1457.5	I(497.0124)	1529.2	1478.4 (1478)	I (405.7)	ν_{as}(C-$(OH)_2$)
1525.1	1442.8	R(17.9002)	1561.2	1508.5 (1519)	R(17.7)	
1768.6	1696.0	R(14.1178)	1728.2	1658.3 (1656)	R(8.0)	ν(C═O)
1838.6	1788.1	I(1039.5765)	1797.0	1751.9 (1752)	I(1149.0)	
3032.2	2516.9	R(227.7607)	3119.5	2684.5 (2752)	R(245.4)	ν(O−H)
3157.1	2741.6	I(3152.0443)	3231.2	2878.9 (2883)	I(2945.8)	
3799.2	3605.2	I(175.9545)	3808.4	3626.7 (3624)	I(189.4)	ν(O−H) (T)
3799.4	3605.3	R(155.2226)	3808.7	3627.0 (3624)	R(123.3)	

[a]Letter T stands for modes due to terminal atoms. The data is from B3LYP/6-311G(2d,d,p) level of theory. [b]Values in parentheses are anharmonic values reported by Tossell using same method, B3LYP/6-311d(2d,d,p).[23]

stretching motion in both cases. Values reported by Tossell are between those calculated here at B3LYP and MP2 levels of theory.

As stated earlier, harmonic frequencies up to a tetramer have been obtained through MP2 calculations. At the MP2 level, anharmonic frequencies are reported here for the monomer and for the anti−anti dimer. Values of frequencies from B3LYP and MP2 levels of theory are comparable; hence, in the rest of the manuscript, we discuss the anharmonic data obtained from B3LYP calculations up to an octamer, unless otherwise stated explicitly.

Harmonic and anharmonic frequencies along with the mode assignments for dimers a and b are provided in Table 3. In both dimers, the C═O bond is elongated and its stretching frequency is red-shifted compared with that in the monomer. While the hydrogen bond (H-bond) length and angle in dimer a are 1.615 Å and 177.1°, the corresponding values in dimer b are 1.643 Å and 177.5°. Thus the H-bonds in dimer a are stronger than those present in dimer b. As the strength of the hydrogen bond increases, the C═O stretching frequency is expected to decrease. This can seen from Tables 2 and 3, where the C═O peak is red-shifted by 58.4 and 56.9 cm^{-1} upon dimerization of a-s monomer (dimer a) and a-a monomer (dimer b), respectively, at the anharmonic level. The activities of vibrational modes are shown in columns 3 and 6 of Table 3, where R and I stand for Raman active and IR active, respectively. Values in parentheses refer to intensities of the corresponding modes. The anharmonic frequencies of dimer b are also compared with those obtained by Tossell[23] in column 5 of Table 3. Since the level of calculation of frequencies is the same in both cases, frequencies calculated here are in good agreement with those of Tossell.[23] The marginal difference between the two sets of data is likely due to the "very tight" convergence that was used in our calculations.

Loerting et al. carried out matrix isolated gas phase vibrational spectroscopy of CA recently.[29] They showed that the gas phase of carbonic acid consists of 90% of anti−anti monomer with the remaining matter constituted by the anti−syn monomer and dimer b species.[29] The infrared spectra of anti−anti and anti−syn monomers and of dimer b are compared against this data in Table S2 of Supporting Information. In the experimental spectrum, a peak corresponding to the out-of-plane bending motion of the CO_3 group appears at 785, 794, and 808 cm^{-1}. In the calculated spectrum, the corresponding peaks are present at 787.0, 773.8, 794.4 cm^{-1} for the anti−anti monomer, anti−syn monomer, and dimer b, respectively. Peaks at 1175 and 1182 cm^{-1} are assigned to the antisymmetric stretching of $C(OH)_2$ and the bending of C(OH) groups. The corresponding mode frequencies are 1109.3, 1127.8, and 1205.8 cm^{-1} for the two monomers and dimer b, respectively. Note that the peak present in dimer b is closer to the experimental value. The in-plane bending of the C(OH) group and the stretching mode of C═O show a peak at 1270 cm^{-1} in the experiment. In our calculations, this mode occurs at 1259.1 cm^{-1}. Peaks corresponding to the stretching of C═O and O−H groups match with those of the anti−anti monomer, anti−syn monomer, and dimer b as shown in Table S2 of Supporting Information. It is to be noted that the C═O and O−H mode frequencies calculated using B3LYP/6-311G(2d,d,p) are comparable to values reported by Tossell or MP2/6-311G(2d,d,p) data.[23]

dx.doi.org/10.1021/jp209715x | J. Phys. Chem. A 2012, 116, 1638−1647

Hydrogen bonding between monomers impacts the vibrational spectrum of the dimer in a significant manner. For instance, the C═O stretch mode present at 1808.8 cm^{-1} in the monomer is red-shifted to values of 1658.3 and 1751.9 cm^{-1} in the dimer (dimer b). The same mode is further red-shifted to 1596.4 and 1643.1 cm^{-1} in the case of the tetramer. The mode frequency is largely unchanged in higher oligomers because the number of hydrogen bonds made by the carbonyl oxygen saturates to a value of two for the tetramer and higher oligomers. Within the harmonic approximation, the IR active C═O stretching mode exhibits peaks at 1851 (monomer), 1797 (dimer b), 1704 (tetramer), 1674 and 1737 (hexamer), and 1663 and 1700.9 and 1749 cm^{-1} (octamer). Since the C═O stretch frequency is nearly the same for oligomer sizes beyond (and including) the tetramer, one can safely compare the features of the octamer spectra against the experimental data for the α and β forms of CA.

The O−H stretch frequency decreases with increasing H-bond strength. The frequencies for dimer b and dimer a are 2684.5, 2878.9 cm^{-1} and 2516.9, 2741.6 cm^{-1} respectively. Both dimers exhibit the center of inversion symmetry in their point group. This property leads to the mutual exclusion of IR and Raman active modes, which can be seen clearly in Table 3. Atomic displacement for all the vibrational modes of dimer b are shown in Figure 2. The vibrational spectrum of the dimer

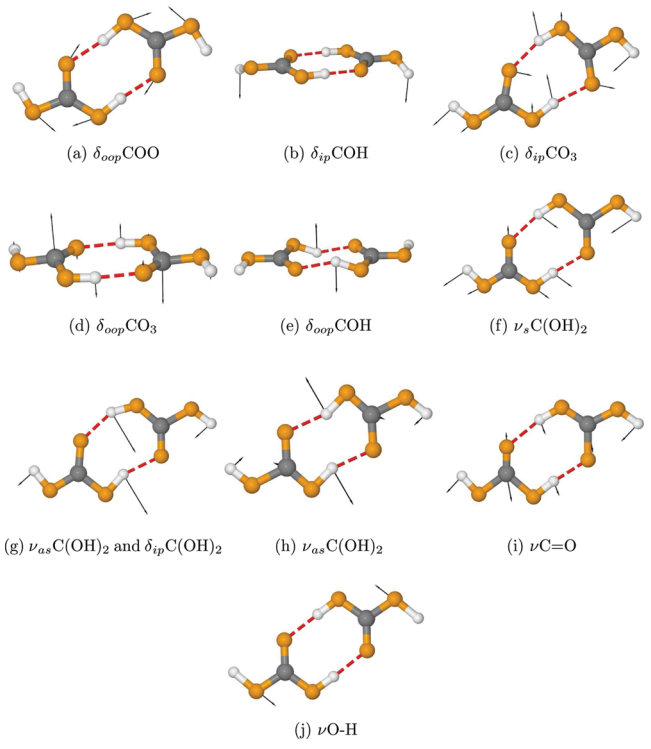

Figure 2. Atomic displacement vectors of various vibrational modes of dimer b (a-a dimer). Hydrogen bonds are shown as red dashed lines, and the vectors are black in color. Color code: C, gray; O, orange; H, white.

contains some features that correspond to intramolecular modes involving the terminal atoms. Their influence (and the IR or Raman intensities) can be decreased if one studies the spectra of large oligomers. It is for this reason that we examine the vibrational spectrum of the linear octamer constituted by the anti−anti conformer.

MP2 calculations using a large basis set such as the one employed here can yield accurate information on bond frequencies. However, they are computationally demanding. Hence, we have carried out harmonic frequency calculations at the MP2/6-311G(2d,d,p) level for the dimer and the tetramer only. The data are compared against those obtained from B3LYP/6-311G(2d,d,p) level of theory (Tables 4 and 5). As seen in Tables 4 and 5, in both cases, the frequencies calculated from the two methods differ only for a few high-frequency modes (mostly bond stretches). Scaling factors (i.e., the ratio of anharmonic to harmonic frequency values at a particular level of theory) can be used to identify systematic errors. Although these are, in general, lower for MP2 than for the B3LYP level of theory,[39] the scale factors for MP2 are not too far off from those for B3LYP. Hence, we continue to discuss the spectral features of the oligomers obtained using B3LYP level of theory against experimental data.

Recently, Loerting and co-workers have measured the infrared and Raman spectra of the two polymorphs of CA and found that while β-carbonic acid has a center of inversion symmetry, the α polymorph does not.[26,32] They also postulated that the β form could contain one-dimensional, hydrogen bonded chains. Experimental observations on α-carbonic acid reveal that the O−H stretch bands are more red-shifted compared with those in the β form.[7] This means either that CA molecules in the α form have stronger hydrogen bonds or that the O−H group in the α-form participates in a higher number of hydrogen bonds compared with those in the β form. Since we have noticed that the a-s dimer (dimer a) forms stronger H-bonds than the a-a dimer (dimer b), it is possible that the α polymorph could consist of carbonic acid molecules in the a-s conformation. They could be in the form of either chains or sheets. However, proton transport in such a crystal could easily transform the conformation from a-s to a-a. Such a phenomenon has earlier been discussed in carboxylic acid crystals.[40] This aspect needs to be investigated in future.

Vibrational frequencies, IR and Raman intensities, and mode assignments of oligomers from trimer up to octamer are given in Tables S3−S8 of Supporting Information.

Comparison with Experimental Data for the Crystals. *Infrared Spectrum.* As mentioned before, anharmonic frequencies for oligomers larger than a tetramer are not reported here, because they exhibit one or more imaginary frequencies at the anharmonic level. Instead, we employed scaling factors to obtain estimates of anharmonic frequencies for the octamer. First, the ratio of anharmonic to harmonic frequencies for each mode of the tetramer was obtained. These ratios (scale factors) were used to obtain the anharmonic frequencies from the calculated harmonic data of the octamer. Where multiple peaks are observed for a particular mode in the tetramer, the mean of the frequencies was used to obtain the scale factor. Features of the "anharmonic" spectrum thus calculated for the octamer are compared against experimental data in Tables 6 and 7. They show the calculated frequencies along with IR and Raman intensities, the scaling factors employed, and also the experimental frequencies observed for the α- and β-carbonic acid samples.[6,7] In the following discussion, modes localized on the terminal CA molecule are ignored, and only the "bulk" modes are presented. In Table 6, the mode at 660, 674.3, and 680.9 cm^{-1} corresponds to the in-plane bending of the CO_3 group in the octamer. The experimental value for the same mode is present at 583 cm^{-1} for the α polymorph and at 661 and 683 cm^{-1} for β-carbonic

dx.doi.org/10.1021/jp209715x | J. Phys. Chem. A 2012, 116, 1638−1647

Table 4. Comparison of Unscaled Harmonic and Anharmonic Frequencies of the anti−anti Dimer (Dimer b) Obtained at B3LYP/6-311G(2d,d,p) and MP2/6-311G(2d,d,p) Levels of Theory[a]

B3LYP		MP2		
har	anhar	har	anhar	assignment
572.7	565.5	575.7	555.7	δ_{ip}(COO)
576.0, 577.6	572.7, 574.2	577.2, 578.3	556.8, 570.8	δ_{oop}(COH)
604.8	598.1	605.8	598.9	
642.7, 653.9	639.6, 649.5	644.7, 652.6	639.1, 646.6	$\delta_{ip}(CO_3)$
802.4, 804.0	793.5, 794.4	805.6, 808.0	798.5, 799.5	$\delta_{oop}(CO_3)$
923.9, 971.9	899.0, 948.2	911.9, 965.1	861.6, 923.4	δ_{oop}(COH)
1025.2, 1031.9	1006.1, 1012.8	1033.8, 1041.8	1014.0, 1023.3	$\nu_s(C(OH)_2)$
1237.4, 1242.5	1202.3, 1205.8	1261.1, 1264.2	1219.7, 1222.2	$\nu_{as}(C(OH)_2)$ and δ_{ip}C(OH)
1390.6, 1392.2	1343.0, 1348.7	1413.3, 1415.5	1374.0, 1380.8	δ_{ip}(COH) and ν(C═O)
1529.2, 1561.2	1478.4, 1508.5	1554.6, 1585.2	1506.3, 1534.4	ν_{as}(C-$(OH)_2$)
1728.2, 1797.0	1658.3, 1751.9	1784.1, 1843.5	1742.0, 1800.7	ν(C═O)
3119.5, 3231.2	2684.5, 2878.9	3318.0, 3414.9	3018.7, 3141.0	ν(O−H)
3808.4, 38087	3626.7, 3627.0	3871.2, 3871.6	3684.9, 3685.4	ν(O−H) (T)

[a]Letter T stands for modes due to terminal atoms.

Table 5. Comparison of Unscaled Harmonic Frequencies of Tetramer Obtained at B3LYP/6-311G(2d,d,p) and MP2/6-311G(2d,d,p) Levels of Theory[a]

B3LYP	MP2	assignment
577.4, 577.6	576.2, 576.3	δ_{oop}COH (T)
581.2, 582.8	585.9, 587.2	δ_{ip}COO (T)
626.5, 658.6	625.9, 656.1	δ_{ip}COO
645.2, 645.3	646.3, 646.7	$\delta_{ip}CO_3$ (T)
669.9, 684.2	670.0, 682.4	$\delta_{ip}CO_3$
798.4, 798.7	802.4, 802.6	$\delta_{oop}CO_3$ (T)
804.4, 805.9	806.7, 809.5	$\delta_{oop}CO_3$
831.0, 880.4, 900.9, 904.3, 957.6, 977.5	831.9, 879.6, 901.5, 902.4, 956.6, 980.1	δ_{oop}C(OH)
1028.7, 1028.7	1038.1, 1038.1	$\nu_s C(OH)_2$ (T)
1058.3, 1065.4	1066.9, 1074.1	$\nu_s C(OH)_2$
1235.3, 1236.2	1259.6, 1260.7	δ_{ip}C(OH) and $\nu_{as}C(OH)_2$ (T)
1354.0, 1359.3	1375.7, 1381.1	δ_{ip}C(OH) and $\nu_{as}C(OH)_2$
1389.1, 1395.5, 1417.1, 1437.2	1414.4, 1419.4, 1444.8, 1464.9	δ_{ip}C(OH) and ν(C═O)
1539.4, 1543.0	1568.3, 1569.4	$\nu_{as}C(OH)_2$ (T)
1579.0, 1602.4	1606.3, 1626.6	$\nu_{as}C(OH)_2$
1663.1, 1704.5	1715.6, 1758.0	ν(C═O)
1773.4, 1786.0	1821.8, 1834.2	ν(C═O) (T)
3142.1, 3142.8, 3225.7, 3243.5, 3310.3, 3364.7	3323.8, 3324.9, 3379.2, 3404.3, 3464.2, 3506.9	ν(O−H)
3807.5, 3807.6	3869.6, 3869.6	ν(O−H) (T)

[a]Letter T stands for modes due to terminal atoms.

acid. The calculated frequencies are in better agreement with the latter than with the former, giving further credence to the idea that the β form is likely to be made up of hydrogen bonded anti−anti conformers organized to form a one-dimensional chain. The out-of-plane bending mode of the CO_3 group is observed at 808.1, 809.8, and 811.4 cm^{-1} for the octamer. These values are close to the experimental data of both the α and β forms. The out-of-plane bending motion of C(OH) group occurs over a broad range of frequencies, 807−958.9 cm^{-1}. The peak with the highest intensity is present at 958.9 cm^{-1}, which is about 40−60 cm^{-1} shifted relative to the experimental data. The out-of-plane motion may be modulated by interchain interactions, which have not been taken into account in the current calculations. Peaks present at 1039.0, 1042.7, and 1048.7 cm^{-1} correspond to the symmetric stretching of the $C(OH)_2$ group in the octamer. The corresponding mode in the experimental spectrum of β-carbonic acid is close to these values, while the mode in α-carbonic acid is present at a higher frequency of 1084 cm^{-1}.

A mode involving both the in-plane bending of C(OH) and the asymmetric stretching of $C(OH)_2$ exhibits a very strong peak at 1303.5 cm^{-1} in the octamer. This mode frequency also is much closer to that for the β crystal rather than that for the α form. In the former, it is present at 1297 cm^{-1}.[7] However, in α-carbonic acid, it is observed at a frequency around 120 cm^{-1}[17] larger than the calculated value. Peaks corresponding to the asymmetric stretching of $C(OH)_2$ group are present at 1501.7, 1517.4, and 1542.6 cm^{-1} in the octamer. Among these, the peak at 1501.7 cm^{-1} is more intense. The corresponding peak for β-CA is at 1501 cm^{-1}, which matches with that of the octamer. However, this mode is present at 1304 and 1477 cm^{-1} in α-carbonic acid.[6] The calculated IR vibrational spectrum for the octamer has no peaks at 1304 cm^{-1}, indicating that the α-form is unlikely to be composed of hydrogen bonded linear chains of the anti−anti conformer.

dx.doi.org/10.1021/jp209715x | J. Phys. Chem. A 2012, 116, 1638−1647

Table 6. Spectral Features in the Infrared Spectrum of the Octamer (Calculated) and in the α and β Forms of Carbonic Acid (Experimental)[6,7a]

		frequency (cm^{-1})		
mode	scaling factor	octamer	α	β
$\delta_{ip}COO$	0.9849	607.5 (6.3), 631.5 (37.9)		
		655.5 (114.4)		
$\delta_{ip}CO_3$	0.9897	660.0 (12.4), 674.3 (50.5)	583	661, 683
		680.9 (305.7)		
$\delta_{oop}CO_3$	1.0076	808.1 (1.1), 809.8 (5.7), 811.4 (47.1)	801	812
$\delta_{oop}C(OH)$	0.9817	807.0 (20.6), 851.5 (25.9), 857.1 (1.6), 875.0 (20.2), 902.9 (16.4), 939.5 (44.8), 958.9 (1389.3)	920	880–900
$\nu_s C(OH)_2$	0.9837	1039.0 (17.0), 1042.7 (0.7), 1048.7 (0.4)	1084	1036
$\delta_{ip}COH$ and $\nu_{as}C(OH)_2$	0.9711	1303.5 (3120.0), 1312.2 (2.0), 1329.8 (159.8), 1351.4 (51.5)	1420	1297
$\delta_{ip}C(OH)$ and $\nu C{=}O$	0.9679	1367.8 (7.8), 1373.2 (7.0)		
$\nu_{as}C(OH)_2$	0.9605	1501.7 (1573.5), 1517.4 (114.0), 1542.6 (8.9)	1304, 1477	1501
$\nu C{=}O$	0.9620	1600.6 (10.3), 1636.3 (58.5), 1682.7 (1191.1)	1715	1700
$\nu O{-}H$	0.9109	2854.4 (3079.9), 2914.2 (7859.5), 2929.5 (4354.1), 2948.2 (3523.2), 3007.9 (1003.5), 3053.9 (245.2), 3084.2 (2855.3)	2585, 2694	2500–3500 2600–3200[b]

[a]The calculations are performed at B3LYP/6-311G(2d,d,p) level of theory. Each mode of the octamer is scaled by a factor given in column 2 to take into account the anharmonicity of the mode. See text for discussion. Values in parentheses denote the IR intensities in arbitrary units. [b]From ref 11.

Table 7. Spectral Features in the Raman Spectrum of the Octamer (Calculated), and in α and β Forms of Carbonic Acid (Experimental)[26,32a]

		Raman shift (cm^{-1})		
mode	scaling factor	octamer	α	β
$\delta_{ip}COO$	0.9849	601.9 (15.5), 618.3 (1.3), 644.4 (5.0), 652.0 (5.3)	681	605, 657
$\delta_{ip}CO_3$	0.9897	667.2 (0.3), 679.4 (0.03)	558, 567	
$\delta_{oop}CO_3$	1.0076	808.2 (0.07), 808.5 (0.3), 809.8 (0.6)	799	
$\delta_{oop}C(OH)$	0.9817	793.3 (1.2), 827.89 (0.1), 865.67 (0.02), 871.2 (0.02), 895.3 (0.2), 920.6 (0.08), 954.5 (0.2)	928	
$\nu_s C(OH)_2$	0.9837	1040.3 (0.9), 1045.7 (6.8), 1050.9 (92.0)	1093	1051
$\delta_{ip}COH$ and $\nu_{as}C(OH)_2$	0.9711	1296.0 (0.4), 1318.2 (0.4), 1329.4 (0.8), 1348.8 (2.1)	1203	
$\delta_{ip}C(OH)$ and $\nu C{=}O$	0.9679	1368.6 (0.9), 1381.4 (6.4), 1401.1 (57.0)		1401
$\nu_{as}C(OH)_2$	0.9605	1505.6 (1.1), 1530.7 (7.0), 1550.6 (38.3)	1427, 1447	1530
			1465, 1489	
$\nu C{=}O$	0.9620	1586.8 (52.3), 1617.0 (2.1), 1659.2 (0.8)	1630	1607
$\nu O{-}H$	0.9109	2855.3 (500.5), 2914.9 (409.6), 2926.4 (272.2), 2946.4 (541.3), 2986.3 (1042.8), 3029.8 (36.0), 3073.0 (10.5)	2976, 3039, 3057	

[a]The calculations are performed at B3LYP/6-311G(2d,d,p) level of theory. Each mode of the octamer is scaled by a factor given in column 2 to take into account the anharmonicity of the mode. See text for details. Values in parentheses denote the Raman intensities in arbitrary units.

As discussed earlier, the symmetric stretching of the C=O bond occurs at 1600.6, 1636.3, and 1682.7 cm^{-1} in the octamer. Among these, the peak at 1682 cm^{-1} is more intense compared with other peaks. This value is very close to the corresponding mode in both the α and β forms (1715 and 1700 cm^{-1}, respectively). The stretching of the O–H bond has a broad range of values between 2854 and 3084 cm^{-1} as given in Table 6. For the α polymorph, this mode shows peaks at 2585 and 2694 cm^{-1}, and in β, this mode shows a broad peak between 2500 and 3500 cm^{-1}. The calculated peak positions compare very well with the spectrum for β, while there is no overlap between the peak positions of α-CA and those calculated for the octamer. From the above analyses, it is clear that the linear octamer spectrum matches well with that of β-carbonic acid. The frequencies of the octamer are also shown as blue sticks in Figure 3. One can see many groups of sticks with each group representing a vibrational mode that has been described above.

To summarize, the following mode frequencies of the octamer match well with the β form exclusively: $\delta_{ip}CO_3$, $\delta_{oop}CO_3$, $\delta_{oop}C(OH)$, $\nu_s C(OH)_2$, $\delta_{ip}C(OH)$, $\nu_{as}C(OH)_2$, $\nu C{=}O$, and $\nu O{-}H$. Yet there are minor differences between these

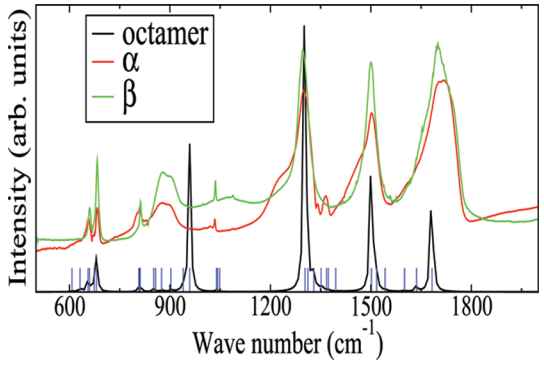

Figure 3. Comparison of the infrared spectra of the linear octamer (calculated) against experimental spectra of α and β forms of carbonic acid.[6,7] Peaks due to terminal atoms are not shown. Calculated frequencies of the octamer are also shown as sticks (blue color).

dx.doi.org/10.1021/jp209715x | J. Phys. Chem. A 2012, 116, 1638–1647

two spectra. In β-carbonic acid, the out-of-plane bending of the C(OH) group has a broad feature between 790 and 950 cm^{-1}.[7] It exhibits two peaks at 881 and 910 cm^{-1} over this broad feature. In the case of the octamer, there are peaks at 807.0, 851.5, 875.0, and 939.5 cm^{-1}, in addition to the one at 958.9 cm^{-1}. Thus, the difference between the calculated and experimental values for this mode frequency is about 58 cm^{-1}. This large difference is likely due to the following reasons: A part of it could come from methodological deficiencies and another from interchain interactions. Anharmonic frequencies corresponding to this out-of-plane mode based on MP2/6-311(2d,d,p) calculations of the dimer and tetramer yield nearly the same frequencies as the B3LYP calculations for the octamer. Hence, we attribute the difference in the frequency of the $\delta_{oop}C(OH)$ mode against experimental data to the lack of interchain interactions in the former. In particular, interchain interactions would shift the calculated frequency for out-of-plane modes to lower values, closer to the experimental data.

In the octamer, a mode ascribed to both the in-plane bending of COH and the stretching of C═O appears at 1367.8, 1373.2, and 1395.2 cm^{-1}, whereas no such peak is seen in the experimental IR spectra of both the α and β forms. However, as can be seen in Table 6, the IR intensities of these peaks are very small, and hence this difference is likely to be insignificant.

Peaks at 607.5, 631.5, and 655.5 cm^{-1} seen in the octamer spectrum correspond to the in-plane bending of the COO group. Among these, the peak at 655.5 cm^{-1} is the most intense. As seen from the table, no corresponding peak is reported in the experiment for either of the polymorphs. However in β-carbonic acid, peaks at 661 and 683 cm^{-1} are assigned to the in-plane bending mode of CO_3 group.[7] Among these, the peak at 683 cm^{-1} is more than twice as intense compared with the peak at 661 cm^{-1}. Since these two modes are quite close to each other, they may have been assigned to the same mode ($\delta_{ip}CO_3$) in the experiment. In the calculated spectrum, the feature at 680.9 cm^{-1} is again twice as intense as the one at 655.5 cm^{-1}. Based on visualization of the atomic displacements, we assign the 655.5 cm^{-1} mode to $\delta_{ip}COO$ and the 680.9 cm^{-1} to $\delta_{ip}CO_3$.

To summarize, the calculated IR modes observed in the octamer match well with those of β-carbonic acid as can be seen in Figure 3.

Raman Spectrum. The calculated Raman spectrum of the octamer is compared against the experimental Raman spectra of α- and β-carbonic acid[26,32] in Table 7. Octamer frequencies are scaled by factors given in column 2, which are the same as in Table 6. For the COO in-plane bending mode, strong peaks are seen at 601.9, 644.4, and 652.0 cm^{-1} for the octamer. For β-CA, this mode is observed at 605 and 657 cm^{-1}, while in the α form it is present at 681 cm^{-1}.[6,7] In the octamer, the peak at 601.9 cm^{-1} has the maximum intensity compared with other peaks for the mode. The same behavior is observed in the corresponding spectrum of β-carbonic acid. The symmetric stretching mode of $C(OH)_2$ exhibits peaks at 1045.7 and 1050.9 cm^{-1} in the octamer and at 1051 and 1093 cm^{-1} in the β and α forms, respectively. The in-plane bending of the COH group and the stretching of the C═O bond are present at 1381.4 and 1401.1 cm^{-1} in the octamer and at 1401 cm^{-1} in β-carbonic acid. It is pertinent to note that this mode is not observed in the experimental spectrum of the α-form. In the spectrum of the octamer, the peaks corresponding to the asymmetric stretching of $C(OH)_2$ are present at 1530.7 and 1550.6 cm^{-1}, which matches well with that in β-carbonic acid; however, in the α form, they are shifted to lower wave numbers. In the octamer, the stretching of the C═O bond exhibits peaks at 1586.8 and 1617.0 cm^{-1}, which agrees well with the peak positions of the corresponding mode in β-carbonic acid (at 1607 cm^{-1}).[7] In the α form, this peak is observed at 1630 cm^{-1}.[6] The quantity $\delta\nu$(C═O) is defined as the difference in the peak positions of Raman and IR frequencies of the C═O stretching mode. Its value is 96.0 cm^{-1} for the octamer, which is comparable to the values of 93.0 and 85 cm^{-1} for α- and β-carbonic acid, respectively.[6,7] Other Raman active modes present in the octamer have very low intensities, and these are not observed in the experimental spectrum of β-carbonic acid. The calculated Raman spectrum of the octamer is compared against the experimental data for α- and β-carbonic acid in Figure 4. The

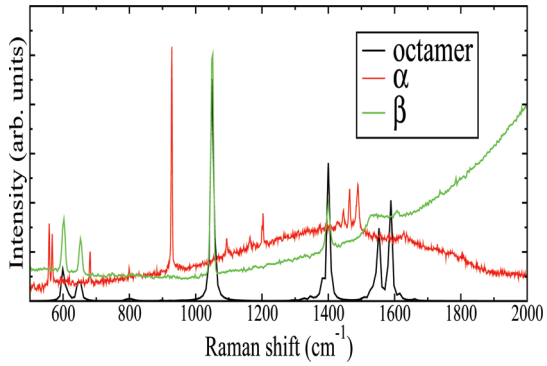

Figure 4. Comparison of the Raman spectra of the linear octamer (calculated) against experimental spectra of α and β forms of carbonic acid.[26,32] Peaks due to terminal atoms are not shown.

main distinction between the Raman spectra of the α and β forms is the peak at 920 cm^{-1}, which is observed in the α form only. This is assigned to out-of-plane bending of the COH group. Not unsurprisingly, this peak is not observed in the calculated spectrum of the octamer. Thus, the Raman data too adds credence to the notion that the β-carbonic acid is likely to be composed of linear hydrogen bonded carbonic acid molecules.

Anti–Syn Oligomers. One dimensional chains formed from a-s conformers were also examined. A linear tetramer, consisting of two dimer a molecules connected to each other with two weak hydrogen bonds (shown as Figure S5 of Supporting Information) is found to be less stable than the linear tetramer made of a-a conformers by 9.2 kcal/mol calculated at B3LYP/6-311G(2d,d,p) level of theory. The linear tetramer formed by s-s conformers can be ruled out based on the large energy difference between the s-s monomer and other conformers. Thus, the one-dimensional chain formed by a-a conformers is the most stable, and the vibrational analysis carried out shows that the anharmonic vibrational spectrum of the octamer matches extremely well with the experimental IR and Raman spectra of β-carbonic acid. In α-carbonic acid, peaks at frequencies 583, 1420, 2585, and 2694 cm^{-1} are either red- or blue-shifted by about 100 cm^{-1} compared with values calculated for the linear a-a octamer. Further, the peaks at 920 and 1304 cm^{-1} present in the spectrum of the α-form are entirely absent in the calculated Raman and IR spectra of the a-a octamer, respectively.

Based on our earlier work on candidate crystal structures for the β-polymorph, the distance between these parallel chains

dx.doi.org/10.1021/jp209715x | J. Phys. Chem. A 2012, 116, 1638–1647

was calculated to be 3.13 Å.[34] We also found that the infrared spectrum of these crystals did not change much from that obtained from a linear oligomer in gas phase, employing the same DFT methods. Double proton transfer between carboxylic acid dimers is a very well-known phenomena and was studied comprehensively using experimental and theoretical methods.[40] Transfer of protons between carboxylic acids is aided by hydrogen bonding. Since carbonic acid molecules exhibit strong hydrogen bonds, double proton transfer between these molecules, which allows them to switch from one conformation to another in the crystalline phase, cannot be ruled out. Such an event in the a-a oligomer would shift the C═O and O−H stretching frequencies to higher and lower wave numbers, respectively.

A Note on Low-Frequency Vibrations. Intermolecular modes dominate in the low-frequency region. The environment around the oligomer, interchain interactions, and anharmonicity are expected to play significant roles in this region. Keeping these limitations in our calculations in mind, we compare the estimated anharmonic spectrum obtained for the octamer against experiment.

Figure 5 shows the far-IR spectrum. The peak centered at 239.3 cm^{-1} corresponds to the rocking motion of CA

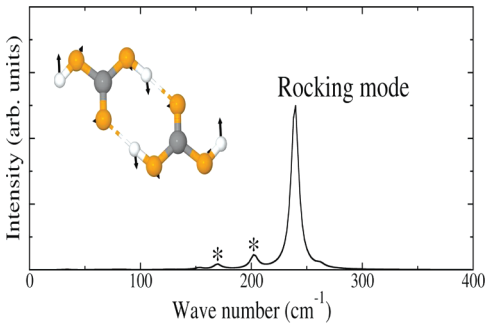

Figure 5. Calculated far-infrared spectrum of the linear octamer of carbonic acid. Atomic displacements observed for the mode at 239.3 cm^{-1} for a dimer is shown as inset. Color code: C, gray; O, orange; H, white. Peaks denoted by asterisks are from terminal molecules in the oligomer.

molecules, whereas the small feature at 202 cm^{-1} corresponds to the same mode due to terminal molecules present in the octamer. Further, a floppy mode is seen at 169 cm^{-1} due to terminal molecules. The intensity of the peak at 239.3 cm^{-1} is very high and is the only one observed above 200 cm^{-1}, which is consistent with our recent ab initio molecular dynamics simulations on chain-like crystal structures.[34] It is to be noted that the experimental low-frequency IR spectra of the α and β forms have not been reported yet.

Figure 6 shows the calculated low-frequency Raman spectrum of the octamer along with the experimental data for α and β forms.[32] Frequency values are also shown as blue sticks. Peaks at 120.6, 125.2, and 136.2 cm^{-1} in the calculated spectrum correspond to out-of-plane bending of the hydrogen bond. Peaks at 165.9, 172.2, and 178.6 cm^{-1} are assigned to intermonomer stretching of CA molecules, whereas the one at 248.8 cm^{-1} corresponds to the in-plane bending of the hydrogen bond. As mentioned before, the rocking motion of CA molecules exhibits peaks at 254 and 259.3 cm^{-1}. The low-frequency Raman spectrum of β-carbonic acid shows peaks at 125, 138, 144, 165, 176, 192, and 258 cm^{-1}.[32] Based on B3LYP

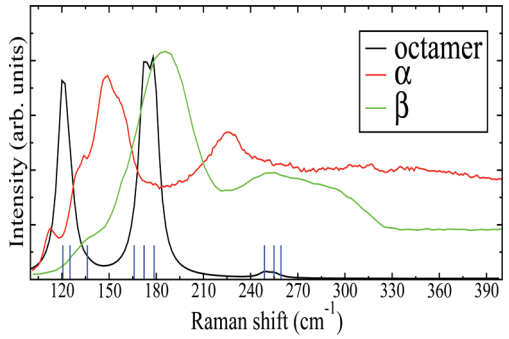

Figure 6. Comparison of the low-frequency Raman spectrum of the linear octamer (calculated) with the experimental spectra of α- and β-carbonic acid.[26,32] Features of the octamer spectrum are also shown as blue sticks.

and MP2 levels of theory calculations using 6-31+G(d) or aug-cc-pVDZ basis sets of the anti−anti dimer, Loerting et al. assigned peaks at 165, 176, and 192 cm^{-1} to intermonomer stretching mode.[32] These features can be seen in Figure 6 where we also show the Raman spectrum calculated by us for the octamer. The octamer spectrum shows features at 165.9, 172.2, and 178.6 cm^{-1}. Based on visualization of atomic displacements, we assign these peaks to intermonomer stretching. As discussed earlier, the peak observed at 258 cm^{-1} in experiments is due to the rocking motion of CA molecules. The peak at 125 cm^{-1} in the β form could be assigned to out-of-plane bending of the hydrogen bond, based on our calculations for the octamer. In general, features below 200 cm^{-1} in the calculated spectrum are red-shifted by about 15−30 cm^{-1} when compared with the experimental data for β-carbonic acid. This shift likely points to the lack of interchain interactions in the present calculations. However, the agreement in the low-frequency region between the calculated and experimental spectra is fair.

4. DISCUSSION AND CONCLUSIONS

We have carried out quantum chemical calculations of oligomers of carbonic acid in gas phase. In particular, linear, hydrogen bonded species of the anti−anti conformation, ranging from a monomer to an octamer were studied for their ground state geometry and harmonic and anharmonic vibrational spectra. Our results for small oligomers (monomer and the dimer) match those obtained by Tossell[23] earlier. In the frequency range higher than 500 cm^{-1}, the calculated infrared and Raman spectra of the octamer agree extremely well with the experimental spectra for β-carbonic acid, rather than with that for the α polymorph.[6,7,26] Our earlier work[34] involved periodic DFT calculations using the PBE functional and AIMD simulations. Here, we have reported vibrational spectroscopic data for gas phase oligomers of linearly hydrogen bonded CA molecules calculated using both MP2 and B3LYP levels of theory. The current calculations add further credence to the postulation that the β form is constituted by chain-like species, possessing a center of inversion. The comparison of the calculated spectrum to experimental results for frequencies below 500 cm^{-1} is fair, pointing possibly to the significance of interchain interactions in modulating the frequencies of modes in this region.

It will now be our endeavor to theoretically investigate the possible structural motifs present in α-carbonic acid.

dx.doi.org/10.1021/jp209715x | J. Phys. Chem. A 2012, 116, 1638−1647

■ ASSOCIATED CONTENT

Supporting Information

Figures showing the oligomers, comparison of vibrational spectra of dimer and tetramer calculated at B3LYP/6-311G(2d,d,p) and MP2/6-311G(2d,d,p) levels of theory, vibrational spectra of oligomers up to size seven, and geometry of all oligomers. This information is available free of charge via the Internet at http://pubs.acs.org.

■ AUTHOR INFORMATION

Notes

The authors declare no competing financial interest.

■ ACKNOWLEDGMENTS

We thank Prof. Thomas Loerting for providing us original experimental data (infrared and Raman spectra) in *x,y* format. The same have been used in Figures 3, 4, and 6 for the sake of comparison. We thank the Department of Science and Technology for support. S.K.R. is grateful to CSIR, India, for a senior research fellowship.

■ REFERENCES

(1) Brucato, J. R.; Palumbo, M. E.; Strazzulla, G. *Icarus* **1997**, *119*, 135.
(2) Strazzulla, G.; Brucato, J. R.; Cimino, G.; Palumbo, M. E. *Planet. Space Sci.* **1996**, *44*, 1447.
(3) DelloRusso, N.; Khanna, R. K.; Moore, M. H. *J. Geophys. Res.* **1993**, *98*, 5505.
(4) Khanna, R. K.; Tossell, J. A.; Fox, K. *Icarus* **1994**, *112*, 541.
(5) Hage, W.; Hallbrucker, A.; Mayer, E. *J. Chem. Soc., Faraday Trans.* **1995**, *91*, 2823. Hage, W.; Hallbrucker, A.; Mayer, W. *J. Mol. Struct.* **1997**, *408*, 527.
(6) Hage, W.; Hallbrucker, A.; Mayer, E. *J. Chem. Soc., Faraday Trans.* **1996**, *92*, 3183.
(7) Hage, W.; Hallbrucker, A.; Mayer, E. *J. Chem. Soc., Faraday Trans.* **1996**, *92*, 3197.
(8) Hage, W.; Liedl, K. R.; Hallbrucker, A.; Mayer, E. *Science* **1998**, *279*, 1332.
(9) Terlouw, J. K.; Lebrilla, C. B.; Schwarz, H. *Angew. Chem.* **1987**, *99*, 352.
(10) Hage, W.; Hallbrucker, A.; Mayer, E. *J. Am. Chem. Soc.* **1993**, *115*, 8427.
(11) Moore, M. H; Khanna, R. K. *Spectrochim. Acta* **1991**, *47A*, 255.
(12) Moore, M. H.; Khanna, R. K.; Donn, B. *J. Geophys. Res. [Planets]* **1991**, *96*, 17541.
(13) Nguyen, M. T.; Raspoet, G.; Vanquickenborne, L. G.; Duijnen, P. Th. V. *J. Phys. Chem. A.* **1997**, *101*, 7379.
(14) Brucato, J. R.; Palumbo, M. E.; Strazzula, G. *Icarus* **1997**, *125*, 135.
(15) Liedl, K. R.; Sekusak, S.; Mayer, E. *J. Am. Chem. Soc.* **1997**, *119*, 3782.
(16) Gerakines, P. A.; Moore, M. H.; Hudson, R. L. *Astron. Astrophys.* **2000**, *357*, 793.
(17) Ballone, P.; Montanari, B.; Jones, R. O. *J. Chem. Phys.* **2000**, *112*, 6571.
(18) Loerting, T.; Tautermann, C.; Kroemer, R. T.; Kohl, L.; Hallbrucker, A.; Mayer, E.; Leidl, K. R. *Angew. Chem., Int. Ed.* **2000**, *39*, 892.
(19) Strazzulla, G.; Baratta, G. A.; Palumbo, M. E.; Satorre, M. A. *Nucl. Instrum. Methods Phys. Res., Sect. B* **2000**, *13*, 166.
(20) Moore, M. H.; Hudson, R. L.; Gerakines, P. A. *Spectrochim. Acta, Part A* **2001**, *57A*, 843.
(21) Tautermann, C. S.; Voegele, A. F.; Loerting, T.; Kohl, I.; Hallbrucker, A.; Mayer, E.; Liedl, K. R. *Chem.—Eur. J.* **2002**, *8*, 66.
(22) Wu, C. Y. R.; Judge, D. L.; Cheng, B.-M.; Yih, T.-S.; Lee, C. S.; lp, W. H. *J. Geophys. Res. [Planets]* **2003**, *108*, 13/1.
(23) Tossell, J. A. *Inorg. Chem.* **2006**, *45*, 5961.
(24) Kumar, P. P.; Kalinichev, A. G.; Kirkpatrick, R. J. *J. Chem. Phys.* **2007**, *126*, No. 204315.
(25) Nguyen, M. T.; Matus, M. H.; Jackson, V. E.; Ngan, V. T.; Rustad, J. R.; Dixon, D. A. *J. Phys. Chem. A* **2008**, *112*, 10386.
(26) Kohl, I.; Winkel, K.; Bauer, M.; Liedl, K. R.; Loerting, T.; Mayer, E. *Angew. Chem., Int. Ed.* **2009**, *48*, 2690.
(27) Tossell, J. A. *Environ. Sci. Technol.* **2009**, *43*, 2575.
(28) Mori, T.; Suma, K.; Sumiyoshi, Y.; Endo, Y. *J. Chem. Phys.* **2009**, *130*, No. 204308.
(29) Bernard, J.; Seidl, M.; Kohl, I.; Liedl, K. R.; Mayer, E.; Galvez, O.; Grothe, H.; Loerting, T. *Angew. Chem., Int. Ed.* **2011**, *50*, 1939.
(30) Loerting, T.; Bernard, J. *ChemPhysChem* **2010**, *11*, 2305.
(31) Mori, T.; Suma, K.; Sumiyoshi, Y.; Endo, Y. *J. Chem. Phys.* **2011**, *134*, No. 044319.
(32) Mitterdorfer, C.; Bernard, J.; Klauser, F.; Winkel, K.; Kohl, I.; Liedl, K. R.; Grothe, H.; Mayer, E.; Loerting, T. *J. Raman Spectrosc.* **2011**, DOI: 10.1002/jrs.3001.
(33) Winkel, K.; Hage, W.; Loerting, T.; Price, S. L.; Mayer, E. *J. Am. Chem. Soc.* **2007**, *129*, 13863.
(34) Reddy, S. K.; Kulkarni, C. H.; Balasubramanian, S. *J. Chem. Phys.* **2011**, *134*, No. 124511.
(35) Frisch, M. J.; Trucks, G. W.; Schlegel, H. B.; Scuseria, G. E.; Robb, M. A.; Cheeseman, J. R.; Scalmani, G.; Barone, V.; Mennucci, B.; Petersson, G. A.; Nakatsuji, H.; Caricato, M.; Li, X.; Hratchian, H. P.; Izmaylov, A. F.; Bloino, J.; Zheng, G.; Sonnenberg, J. L.; Hada, M.; Ehara, M.; Toyota, K.; Fukuda, R.; Hasegawa, J.; Ishida, M.; Nakajima, T.; Honda, Y.; Kitao, O.; Nakai, H.; Vreven, T.; Montgomery, J. A., Jr.; Peralta, J. E.; Ogliaro, F.; Bearpark, M.; Heyd, J. J.; Brothers, E.; Kudin, K. N.; Staroverov, V. N.; Kobayashi, R.; Normand, J.; Raghavachari, K.; Rendell, A.; Burant, J. C.; Iyengar, S. S.; Tomasi, J.; Cossi, M.; Rega, N.; Millam, J. M.; Klene, M.; Knox, J. E.; Cross, J. B.; Bakken, V.; Adamo, C.; Jaramillo, J.; Gomperts, R.; Stratmann, R. E.; Yazyev, O.; Austin, A. J.; Cammi, R.; Pomelli, C.; Ochterski, J. W.; Martin, R. L.; Morokuma, K.; Zakrzewski, V. G.; Voth, G. A.; Salvador, P.; Dannenberg, J. J.; Dapprich, S.; Daniels, A. D.; Farkas, O.; Foresman, J. B.; Ortiz, J. V.; Cioslowski, J.; Fox, D. J. *Gaussian 09*, revision B.01; Gaussian, Inc.: Wallingford, CT, 2009.
(36) Porezag, D.; Pederson, M. R. *Phys. Rev. B* **1996**, *54*, 7830.
(37) Jmol: An open-source Java viewer for chemical structures in 3D. http://www.jmol.org/.
(38) McMahon, B.; Hanson, R. M. *J. Appl. Crystallogr.* **2008**, *41*, 811.
(39) Merrick, J. P.; Moran, D.; Radom, L. *J. Phys. Chem. A* **2007**, *111*, 11683.
(40) Loerting, T; Liedl, K. R. *J. Am. Chem. Soc.* **1998**, *120*, 12595.